Steady circulation induced by inertial modes in a librating cylinder

Stanislav Subbotin *

Laboratory of Vibrational Hydromechanics, Perm State Humanitarian Pedagogical University, 614000 Perm, Russia

(Received 10 September 2019; published 24 January 2020)

The paper is devoted to an experimental study of steady flows excited by an oscillating motion of fluid in a cylinder, the rotation rate of which periodically changes (librations). The rotational oscillations lead to the appearance of a system of averaged toroidal vortices in a viscous Stokes boundary layer close to the cylinder side wall. The number of vortices depends on the frequency of librations, σ. If σ exceeds twice the rotation rate, the steady flow structure has the form of two vortices located close to the cavity ends, i.e., corner flow. If $\sigma < 2$ at some libration frequencies, inertial modes—natural modes of rotating fluid oscillations in the closed cavity—are excited. In this case additional averaged vortices arise. The number of vortices is determined by the axial wave number of the inertial mode. With a decrease in the dimensionless frequency of fluid oscillation, the vortices increase in size, which leads to a transformation of the vortex structure. In this case, the flow near the ends is a superposition of the flows excited by inertial mode and corner flow. At the same time, the vortices which are the most distant from the periphery do not feel the corner flow. It is shown that the viscous dissipation of the oscillating motion in the fluid bulk leads to a linear decrease in the velocity of steady circulation with the dimensionless frequency.

DOI: 10.1103/PhysRevFluids.5.014804

I. INTRODUCTION

It is known that oscillations of viscous fluid near solid walls lead to an occurrence of averaged effects. A classic example is steady streaming [1]. The oscillations result in a dynamic Stokes boundary layer in which averaged shear stresses are generated. The situation changes when the oscillations occur against the background of the rotation. In this case, the Coriolis force acts on the fluid and oscillating Ekman boundary layers appear on the walls that are not parallel to the rotation axis [2]. Nonlinear effects in Ekman layers also lead to the appearance of mean flows [3]. An example of a harmonic forcing on rotating systems is longitudinal librations [4,5]: sinusoidal changes in the rotation rate. The interest of researchers in this area is due to the fact that the libration movement is characteristic of many planetary bodies [6,7]. From a fundamental point of view, the problem of fluid flow in a librating cylinder is no less interesting. In this case, both types of oscillating boundary layers arise at the boundaries: Ekman layers on the end walls and a Stokes layer on the side wall. The first studies of the effect of librations on the fluid flow in a cylindrical geometry were carried out by Wang [8], who showed that rotational oscillations lead to the appearance of retrograde zonal flow. Later, the case of low-frequency librations was theoretically considered by Busse [9]. In theory, the mechanism of zonal flow generation was associated with nonlinear effects in the Ekman layers on the end walls, while the Stokes layer on the side wall of the cylinder was excluded from consideration. In [10] and [11] experimental and numerical confirmation of zonal flow existence in a librating cylinder was given.

*subbotin_sv@pspu.ru

 ©2020 American Physical Society

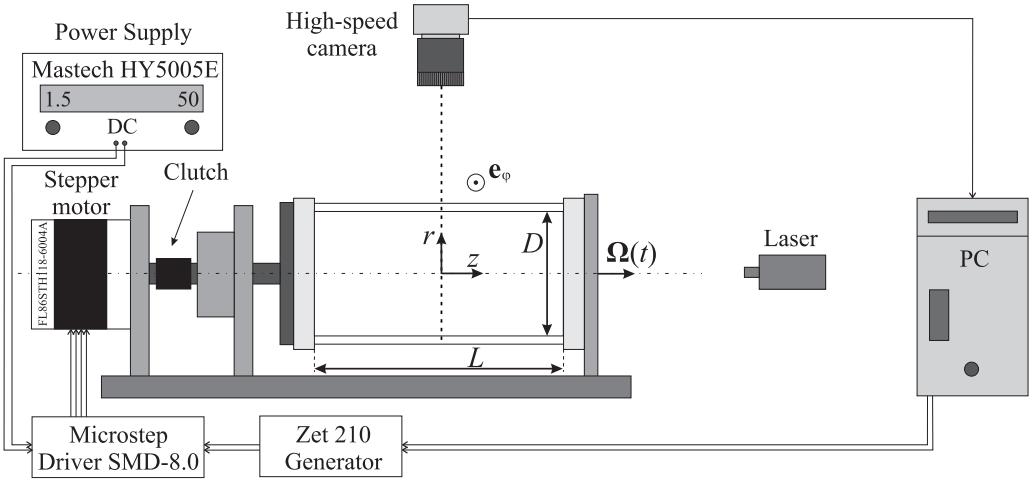

FIG. 1. Scheme of the experimental setup.

If the libration frequency is less than twice the mean rotation rate, in addition to the zonal flow, inertial waves are generated. These waves propagate along the characteristic conical surfaces formed by free shear layers. The direction of wave beam propagation relative to the rotation axis is determined only by the oscillation frequency [2,12]. In closed cavities, at certain libration frequencies, so-called inertial modes are excited. These modes are eigenmodes of a rotating fluid in a given cavity geometry [13–15]. Studies [11,16–18] show that the resonant excitation of the inertial mode is capable of several times intensifying the zonal flow. At the same time, outside the resonant frequencies, the differential velocity of the fluid is significantly lower [17]. As shown in [16] the mechanism of the zonal flow was associated exclusively with nonlinear self-interaction of inertial modes. On the other hand, as experiments [19–21] show, inertial waves and modes are capable of generating steady circulation in dynamic boundary layers. For example in [19] pattern formation, excited by oscillations of the free surface of the centrifuged fluid layer, on the side wall of a rotating cylinder was studied. The heavy particles of the visualizer formed a system of periodic axisymmetric ring structures along the axis of rotation. An analysis of the results showed that the pattern formation is associated with a reflection of the inertial wave beam from the cylinder side wall. Similar azimuthal particle structures associated with the reflection of inertial waves were observed in a spherical cavity, in the center of which was an oscillating spherical core [20]. A study of steady circulation excited by inertial wave beams in a librating cylinder with the help of particle image velocimetry (PIV) was performed in [21]. The case of small amplitudes of rotational oscillations, when centrifugal instability does not occur at the cavity side wall, was considered. It was found that the interaction of the inertial wave with the boundary layer qualitatively changes the two-dimensional structure of the zonal flow. The pulsating motion caused by the reflection of the wave beam leads to the formation of a system of averaged toroidal vortices in the Stokes boundary layer. The vortex motion of the fluid also led to the redistribution of small heavy particles on the side wall in the form of a system of axisymmetric ring structures. Each ring was located between two vortices, forming oncoming flows along the wall. In the present work, the research begun in [21] is extended. The main attention is focused on the study of the structure and velocity of the flow that occurs in the Stokes boundary layers under resonant excitation of the inertial mode in a librating cylindrical cavity.

II. EXPERIMENTAL SETUP AND TECHNIQUE

The experiments are carried out using the equipment schematically presented at Fig. 1. The cavity is a circular cylinder with length $L = 102.0$ mm and radius $R = 26.0$ mm, filled with liquid. The ends of the cavity are closed with Plexiglas flanges and fixed in the ball bearings of the supports.

TABLE I. The values of the parameters in experiments.

Parameter	Definition	Value
L	Cavity length	102.0 mm
$R = D/2$	Cavity radius	26.0 mm
L/R	Aspect ratio	3.92
Ω_{rot}	Mean rotation rate	$15.70-62.80\,\text{s}^{-1}$
Ω_{lib}	Frequency of librations	$9.42-125.6\,\text{s}^{-1}$
ν	Kinematic viscosity of the fluid	7.0−250 cSt
$\Delta\varphi$	Angular amplitude of rotational oscillations	0.03−0.67 rad
$\sigma = \Omega_{\text{lib}}/\Omega_{\text{rot}}$	Dimensionless frequency of librations	0.3−2.0
$\varepsilon = \Delta\varphi\sigma$	Amplitude of librations	0.05−0.20
$E = \nu/(\Omega_{\text{rot}}R^2)$	Ekman number	$10^{-4}-10^{-2}$
$\delta = \sqrt{2\nu/\Omega_{\text{lib}}}$	Stokes boundary layer thickness	0.4−4.8 mm
$\omega = \Omega_{\text{lib}}R^2/\nu$	Dimensionless frequency of fluid oscillations	$60-10^4$

One of the flanges is installed in the bearing, the inner diameter of which exceeds the diameter of the cylinder, which allows observations along the axis of symmetry. To compensate for the optical distortions on the side cylindrical wall, the cavity is placed into a transparent Plexiglas box in the form of a parallelepiped. The space between the cavity and the walls of the box is filled with working fluid. The working fluid is a water-glycerol solution, with kinematic viscosity varying in the range $\nu = 7-250$ cSt in different experiments. A cylindrical coordinate system (r, φ, z) with the origin in the center of the cavity is used.

The case of nonuniform rotation of the cavity is considered. The rate of rotation changes in the laboratory reference frame according to the law

$$\Omega(t) = \Omega_{\text{rot}}(1 + \varepsilon \sin(\Omega_{\text{lib}}t)),$$

where Ω_{rot} is the mean rotation rate of the cavity, Ω_{lib} is the angular libration radian frequency, and $\varepsilon \equiv \Delta\varphi\Omega_{\text{lib}}/\Omega_{\text{rot}}$ is the modulation amplitude of rotational oscillations. As a dimensionless characteristic of the libration frequency, the parameter $\sigma \equiv \Omega_{\text{lib}}/\Omega_{\text{rot}}$ is used. The parameters under which the experiments are performed are given in Table I.

The rotation of the cavity is set by a stepper motor (Fulling Motor FL86STH118-6004A) controlled by a driver (Smart Motor Devices SMD-8.0) and powered by a direct current source (Mastech HY5005E). The main step of the motor equals 1.8° and is divided by 0.45° by the driver. The motor shaft rotation velocity is adjusted using a ZETLAB Zet 210 Sigma USB generator module. The motor shaft is connected to the axis of the cuvette using a clutch that transmits rotation with a high degree of accuracy.

Initially, the cuvette is brought into a rapid uniform rotation about a horizontal axis with the speed of Ω_{rot}. After establishing the solid-state rotation of the fluid, the frequency Ω_{lib} and the amplitude ε of librations are set. The velocity field in an axial section of the cylinder is studied by the PIV method. For this purpose, a small amount of plastic spherical particles with a diameter of $d \sim 60\,\mu$m and average density $\rho \sim 1.05\,\text{g/cm}^3$, are added to the working fluid. The volume fraction of particles in the working fluid does not exceed 10^{-4}. The liquid is illuminated by a light plane created by a continuous laser (Z-Laser Z500Q). Video recording of the position of light-scattering particles is carried out using a high-speed camera (CamRecord CL600×2), which is immovable in the laboratory reference frame. The recording frequency in different experiments varies from 20 to 100 fps, but for analysis only those are selected from the entire sequence of frames such that the time interval between them is a multiple of the mean rotation rate period $2\pi/\Omega_{\text{rot}}$. After this time the same particles of the visualizer are illuminated by the laser (the thickness of the laser sheet is about 2 mm). Since the intensity of zonal flow is small, the movement of one particle along the z axis can be tracked over the time of several revolutions of the cavity. An obtained sequence

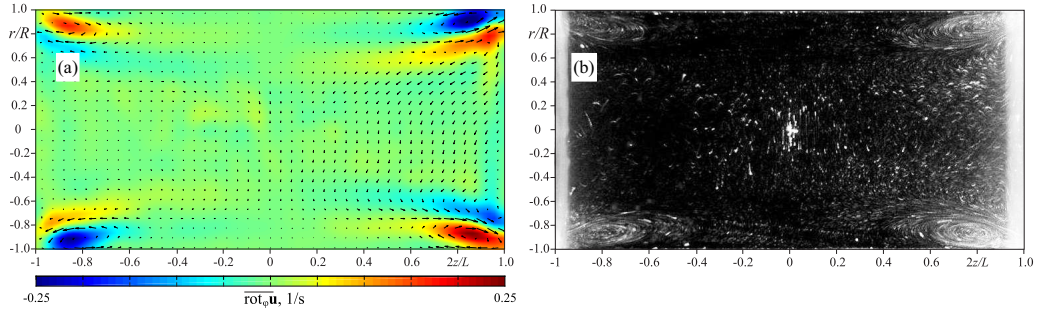

FIG. 2. The velocity field averaged over the period of librations in the axial section of the cylinder (a) and track visualization of the flow structure (b) at $\sigma = 2.2$, $\varepsilon = 0.10$, and $E = 1.8\times10^{-3}$. The color shows the φ component of the averaged vorticity field, $\overline{\mathrm{rot}_\varphi \mathbf{u}}$.

of photos is processed using the program PIVLAB [22], after which the instantaneous and averaged (over the period of librations) velocity fields are studied. Note that the averaged velocity field is calculated over at least ten libration periods. To demonstrate the steady flow structure the track visualization is used. Images are generated by combining frames, the time interval between which is a multiple of the average period.

All the experiments are carried out below the threshold of centrifugal instability on the side wall of the cylinder. The maximum value of Reynolds numbers $\mathrm{Re} = \varepsilon \mathrm{E}^{-3/4} < 250$ [10], where $E = \nu/(\Omega_{\mathrm{rot}} R^2)$ is the Ekman number.

III. EXPERIMENTAL RESULTS

Initially, let us describe a flow structure associated exclusively with rotational oscillations of the cavity ($\sigma > 2$). In this case, an averaged retrograde zonal flow arises. Previous theoretical and experimental studies [4,10,11,21] show that the velocity of this flow is proportional to the square of the libration amplitude. Near a junction of the side and end walls of the cylinder, corner flow is additionally generated (Fig. 2). This flow has the form of two averaged toroidal vortices, in which the fluid moves along the side wall from the ends to the cavity center. As was shown in [21] corner flow exists in the entire range of libration frequencies, and the fluid velocity in vortices also varies with the libration amplitude according to the law $\sim\varepsilon^2$.

In the frequency range $0 < \sigma \leqslant 2$ oscillating fluid motion propagates from the cavity corners into the fluid bulk in the form of inertial waves [2]. The direction of inertial wave beam propagation is determined by a ratio between the libration frequency and twice the mean rotation rate: $\theta = \arcsin(\sigma/2)$. Inertial wave beams generated by cavity librations were studied previously in cavities of various geometries: rotating cylinder [11,21], rotating annulus [14], rotating annulus with a truncated inner cylinder [23], as well as a cubic cavity [13,15]. In all the above works, wave beams were born near the cavity corners, where the Stokes and Ekman boundary layers interact.

At certain libration frequencies, inertial waves excite the inertial modes. These modes are the natural frequencies of oscillations of a rotating fluid and strongly depend on the geometry of the cavity. The natural frequencies of inviscid inertial modes in the cylinder are determined by the following expression:

$$\sigma^2 = \frac{4n^2\pi^2}{n^2\pi^2 + \xi_{nmk}^2 L^2/R^2}, \tag{1}$$

where n is an axial wave number and L/R is the aspect ratio. The parameter ξ_{nmk}^2 is the m positive solution to the transcendental equation

$$\xi \frac{d}{d\xi} J_{|k|}(\xi) + k\left(1 + \frac{\xi^2}{n^2\pi^2 L^2/R^2}\right)^{1/2} J_{|k|}(\xi) = 0, \tag{2}$$

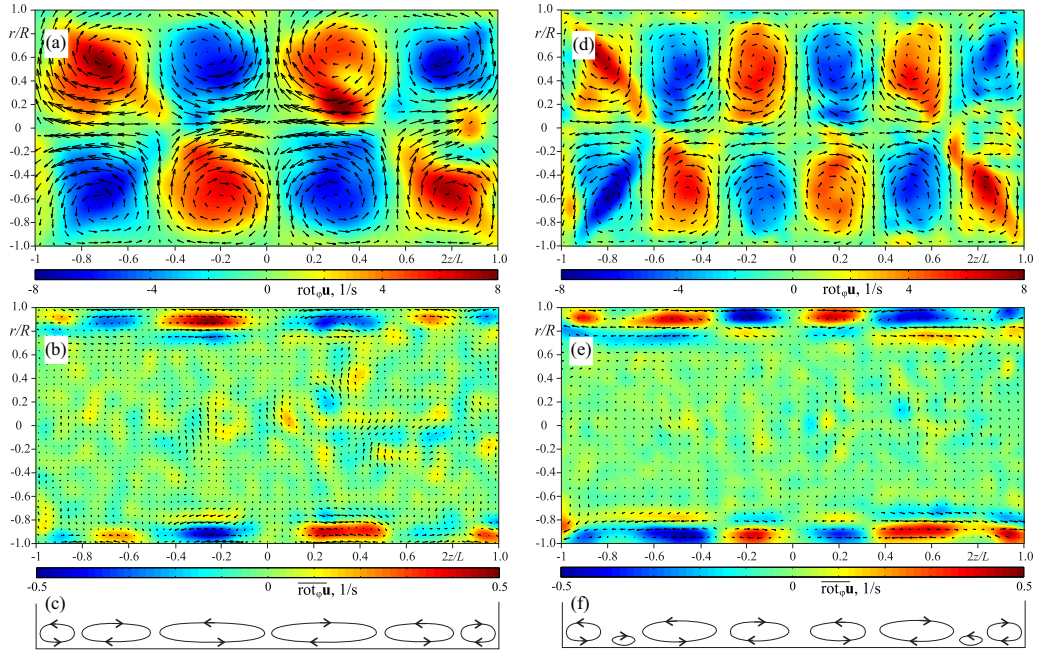

FIG. 3. Instantaneous and averaged velocity field at $\sigma = 1.28$ {4,1} and $\omega = 3900$ (a), (b), and at $\sigma = 1.56$ {6,1} and $\omega = 4700$ (d), (e). The amplitude of librations and the Ekman number are $\varepsilon = 0.12$ and $E = 3.3\times10^{-4}$ respectively. Panels (c) and (f) show the schemes of steady circulation in the Stokes layer.

where $J_{|k|}(\xi)$ is the first kind Bessel function of $|k|$ order. Since an axisymmetric flow is considered, $k = 0$ and only the axial and radial wave numbers $\{n, m\}$ are used for the spatial characteristic of the inertial mode. The ends of the cavity oscillate symmetrically. For this reason, only symmetrical modes arise with respect to the plane $z/L = 0$ with even values of n.

Figures 3(a) and 3(d) show the instantaneous velocity field and corresponding vorticity field for modes {4,1} and {6,1} in the libration phase $\Omega_{\rm lib}t = \pi$. The oscillating flow is a system of toroidal vortices in which the direction of the fluid rotation changes during the libration period. Therefore in the antiphase ($\Omega_{\rm lib}t = 0$) the vorticity will be the opposite. The structure of the oscillating flow depends on the radial wave number m. For example, when a mode {4,2} is excited, the number of vortices doubles. In general, the results of visualization of the instantaneous velocity field by the PIV method are in a good agreement with theoretical predictions [2].

A. Steady circulation

The oscillations of the fluid excited by the inertial mode in the fluid bulk lead to the appearance of a steady circulation in the viscous Stokes boundary layer on the side wall of the cavity. The structure of this flow manifests itself when averaging the velocity field over the period of librations. Figures 3(b) and 3(c) show the averaged velocity field and schematically illustrate the steady circulation corresponding to the mode {4,1}. The flow has the form of a system of toroidal vortices, the size of which along the z axis is consistent with the size of the oscillating vortices. An exception is a region near the junction of the side and end walls, where the flow structure is complicated by the presence of the corner flow. The transverse size of the vortices is limited by several thicknesses of the Stokes boundary layer, $\delta = \sqrt{2\nu/\Omega_{\rm lib}}$, and their number is determined by the expression $n + 2$. Therefore at $n = 6$ [Figs. 3(d)–3(f)] the number of vortices localized in the boundary layers is 8. In this case, the vortices excited by an oscillating motion at the periphery ($|2z/L| > 0.7$) are

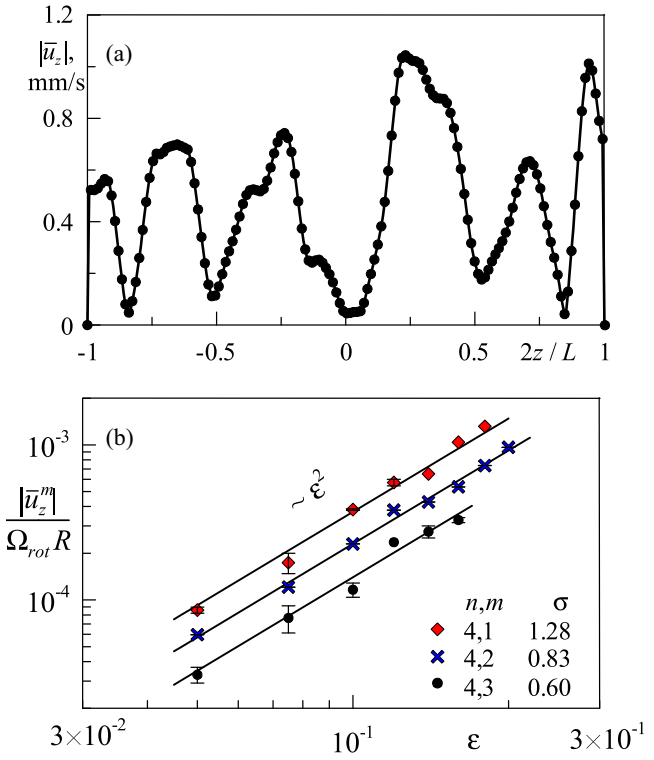

FIG. 4. (a) The distribution of the averaged velocity modulus $|u_z|$ along the cylinder side wall at $\sigma = 1.28$, $\varepsilon = 0.12$, and $E = 1.6\times10^{-4}$; (b) dependence of the maximum fluid velocity in the vortices on the amplitude of librations ε at a fixed value of the axial wave number at $n = 4$ and different values of radial number m.

significantly suppressed by the corner flows of opposite vorticity. These flows are weakly visible on the velocity field [Fig. 3(e)] and schematically depicted as vortices of the smallest size in Fig. 3(f). It should be noted that the number of averaged vortices does not depend on the radial number m. With an increase in m only a change in the intensity of the averaged motion is observed.

The absolute value of the maximum averaged velocity along the side wall of the cavity $|\bar{u}_z^m|$ is taken as a characteristic of the flow rate. Thus, for example, at the frequency $\sigma = 1.28$ (mode $\{4,1\}$) the average velocity at four maxima located in the range $|2z/L| = 0.1-0.9$ is calculated [Fig. 4(a)]. The flows excited by the angular oscillations of the cavity are not taken into account during averaging.

Figure 4(b) shows the dependence of the module maximum fluid velocity $|\bar{u}_z^m|/(\Omega_{\rm rot}R)$ on the amplitude of librations ε. The experiments show that at a fixed frequency σ the intensity of the averaged motion increases according to the law ε^2. The quadratic dependence is determined by the mechanism of steady circulation generation associated with nonlinear effects in the Stokes boundary layers. This result is universal and is in good agreement with the studies of the influence of various types of harmonic effects on rotating systems [3]. Thus, at fixed values of the libration frequency σ and Ekman number E the fluid velocity is completely determined by one dimensionless complex, $V = |\bar{u}_z^m|/(\Omega_{\rm rot}R\varepsilon^2)$.

When there is a change in the libration frequency σ, the averaged velocity V changes nonmonotonically, experiencing a series of extrema corresponding to resonant excitation of an inertial mode with a wave number $\{n, m\}$ (Fig. 5). In this case, the most intensive fluid motion is observed for the main mode $\{2,1\}$, when all the energy is accumulated in two oscillating toroidal vortices. With an increase in the radial wave number m the intensity of the flow rapidly decreases. The next largest

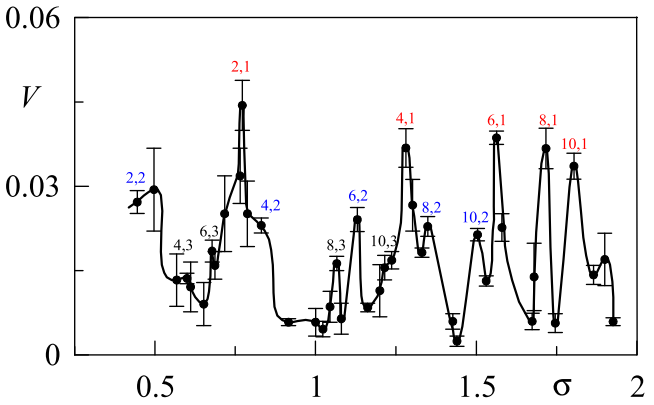

FIG. 5. Distribution of the dimensionless averaged velocity $V = |\bar{u}_z^m|/(\Omega_{\rm rot} R\varepsilon^2)$ over the libration frequency σ at $E = 1.6\times10^{-4}$; labels 2,1, 6,2, etc. mean the numbers of inertial modes $\{n, m\}$.

peaks are associated with resonant mode $\{n, 2\}$ excitation. The value of dimensionless velocity V is about one and a half times less than that for modes with a radial wave number $m = 1$. Finally, the flows related to modes $\{n, 3\}$ practically do not manifest themselves due to the strong viscous dissipation of the small-scale pulsating motion of the fluid in fluid bulk.

A similar dependence on the frequency of external harmonic forcing was obtained in numerical simulations [11] with a librating cylinder with aspect ratio $L/R = 2$ and in experiments [17] with a rotating and periodically deformable spherical cavity. In contrast to the current research, in both works attention was paid exclusively to the zonal flow. Similarly, at a frequency corresponding to one of the inertial modes, the averaged velocity of zonal flow increased in a resonant manner.

B. Effect of the dimensionless frequency ω

The most important parameter of the problem is the dimensionless frequency of fluid oscillations relative to the cavity, $\omega = \Omega_{\rm lib} R^2/\nu$, which characterizes the square of the ratio between the cavity size and the thickness of the Stokes boundary layer δ on the cylinder side wall. In the area of high frequencies ($\omega > 2\times10^3$) the structure of the flow has the form shown in Fig. 3. As the dimensionless frequency decreases, the relative thickness of the boundary layers increases. As a result the size of the averaged toroidal vortices also increases. For example, at a frequency $\sigma = 0.77$ (mode {2,1}) and $\omega = 330$ averaged vortices excited by inertial modes grow up to the cavity end walls, interacting with the corner vortices [Figs. 6(a) and 6(e)]. Thus, close to the cavity ends, the flow is a two-level system consisting of a pair of vortices with opposite vorticity. It is noteworthy that the result is a superposition of two flows due to two different mechanisms: the rotational oscillations of the cavity and resonant oscillations in the fluid bulk.

A transformation of the steady flow structure for mode {4,1} is similar. With a decrease in ω the averaged vortices located at a distance $|2z/L| = 0.6-0.8$ [Fig. 3(b)] increase in size and are displaced to the periphery by expanding central vortices [Figs. 6(b) and 6(f)]. Track visualization of the flow shows that already at $\omega = 540$ averaged vortices in the central part of the cavity reach a significant size, $r/R \approx 0.3$. At the same time, close to the cavity ends the flow structure is a two-vortex system similar to that observed at $\sigma = 0.77$ [Figs. 6(a) and 6(e)].

The evolution of the flow excited by higher-order modes with a change in ω is slightly different. Thus at $\sigma = 1.56$ (mode {6,1}) the vortices located at a distance $|2z/L| = 0.7-0.8$ [Fig. 3(e)] are completely suppressed. As a result, the corner flows are combined with neighboring vortices of the same vorticity, forming one large vortex near the cavity ends [Figs. 6(c) and 6(g)]. Thus, an eight-vortex structure [Fig. 3(e)] is replaced by a four-vortex one [Fig. 6(c)]. Despite the fact that the numbers of averaged vortices close to the side wall at $\sigma = 1.28$ and $\sigma = 1.56$ are identical, the

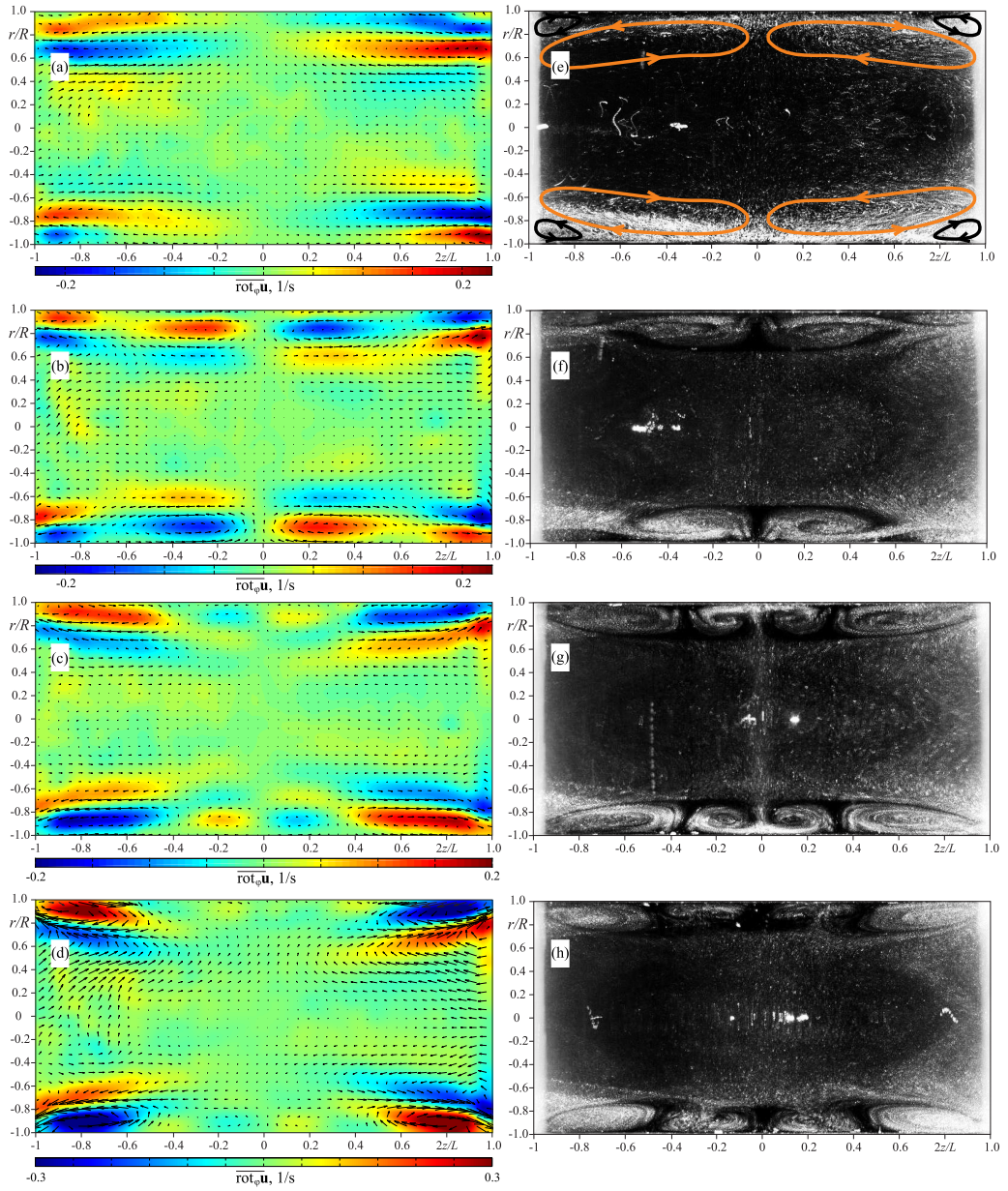

FIG. 6. Averaged velocity field and its track visualization at $\sigma = 0.77$ (mode {2,1}), $\varepsilon = 0.15$, and $\omega = 330$ (a), (e); $\sigma = 1.28$ {4,1}, $\varepsilon = 0.15$, and $\omega = 540$ (b), (f); $\sigma = 1.56$ {6,1}, $\varepsilon = 0.15$, and $\omega = 660$ (c), (g); $\sigma = 1.72$ {8,1}, $\varepsilon = 0.20$, and $\omega = 730$ (d), (h). The Ekman number for all cases is $E = 2.4\times10^{-3}$. In panels (a)–(d) the color shows the φ component of the vorticity field averaged over the libration period, $\overline{\mathrm{rot}_\varphi \mathbf{u}}$; solid curves with arrows in panel (e) schematically illustrate the structure of the steady circulation.

central vortices differ in both the sign of vorticity and size. This is associated with a slight increase in the dimensionless frequency ω for mode {6,1} compared to mode {4,1}. Figure 6(g) shows that the thickness of the central vortices decreases to $r/R \approx 0.2$. The structure of the steady flow for the mode {8,1} is transformed similarly. As a result of the dominance of the corner flow, the ten-vortex flow transforms into a six-vortex one [Figs. 6(d) and 6(h)].

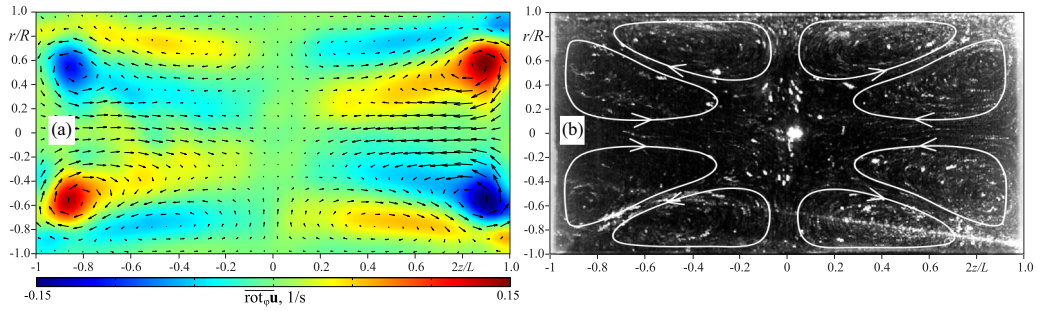

FIG. 7. Averaged velocity field and its track visualization at $\sigma = 1.28$ {4,1}, $\varepsilon = 0.15$, $\omega = 110$, and $E = 1.2\times10^{-2}$.

With a further decrease in ω the averaged flows increase in size and their thickness becomes comparable with the size of the cavity. In the range of frequency $\omega < 10^2$, irrespective of the number of the excited mode, the flow consists of two pairs of coordinately rotating toroidal vortices (Fig. 7). The vortex motion generates a flow in the form of jets directed to the corners. At the same time, the strongest flow directed from the ends of the cavity to its center arises along the axis of rotation. Note that, in the case of zero average rotation ($\Omega_{\rm rot} = 0$), rotational oscillations with frequency $\Omega_{\rm lib}$ generate a vortex motion close to the ends of the opposite vorticity [24,25].

C. Effect of the Ekman number

The dependence of the flow velocity $V = |\bar{u}_z^m|/(\Omega_{\rm rot} R\varepsilon^2)$ excited by the modes {2,1}, {4,1}, and {6,1} on Ekman number $E = \nu/(\Omega_{\rm rot}R^2)$ is shown in Fig. 8. In all cases, with increasing E the fluid motion in the averaged vortices is dissipated by viscosity according to a power law, and the scaling for different inertial modes can differ. In the range of low Ekman numbers ($E < 10^{-3}$) dissipation of oscillating fluid motion in the fluid bulk leads to a decrease in the maximum velocity according to the law $V \sim E^{-1/2}$. However, at $E > 10^{-3}$ a violation of the detected scaling is observed. The monotonic decrease in the intensity of the flow excited by modes {2,1} and {4,1} is replaced by the output of the system at a constant value. It can be assumed that additional energy pumping into the flow is associated with its transformation caused by a change in the dimensionless frequency ω. Indeed, as experiments show [Figs. 6(a), 6(b), 6(e), and 6(f)], the decrease in ω leads to an increase in the size of the vortices. As a result, the flow excited by the

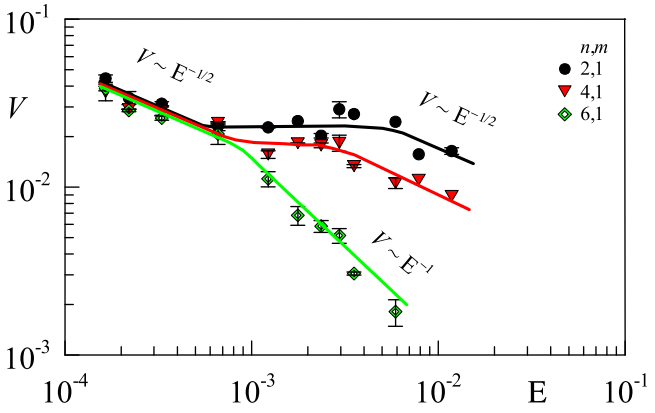

FIG. 8. Dependence of the velocity of steady circulation on the Ekman number E.

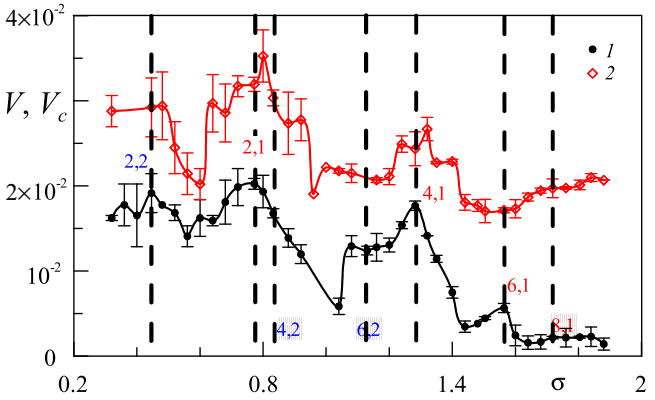

FIG. 9. Dependence of the dimensionless velocity of steady circulation excited by the fluid oscillations in the fluid bulk, V (points: 1), and the velocity of the corner flow, V_c (rhombuses: 2), on the frequency of librations σ at $E = 2.4\times10^{-3}$. Shading indicates the viscosity dissipated modes.

inertial mode begins to strongly interact with the corner flows. After the saturation of the steady flow with additional energy ($E > 3\times10^{-3}$), the monotonic decrease of velocity is renewed according to the law $V \sim E^{-1/2}$.

For mode {6,1} the scaling $V \sim E^{-1/2}$ changes to $V \sim E^{-1}$, which differs from dissipation scaling for modes with lower wave numbers. It should be noted that in this case the velocity was measured only in the central vortices at a distance $|2z/L| = 0.1-0.3$ [Fig. 6(c)]. These vortices are associated exclusively with resonant oscillations of the inertial mode and are not burdened by the influence of corner flow. At the same time, with an increase in E the amplitude of the pulsating motion of the fluid decreases with distance from the ends, and takes the smallest value near the areas where the measurements were made.

Note that in spherical geometry the dependence of the velocity of zonal flow excited by the inertial mode also strongly depends on the oscillation frequency. For example, in the case of tidal oscillations of a sphere with a resonant frequency $\sigma_{\text{tide}} = 0.38$ in the range of Ekman numbers $E = 5\times10^{-5}-10^{-3}$, a scaling in $\sim E^{-3/10}$ was obtained in experiments [17]. Even with a small deviation from the resonance frequency to $\sigma_{\text{tide}} = 0.384$ the scaling had changed significantly $\sim E^{-0.64}$, and at $\sigma_{\text{tide}} = 0.178$ zonal flow velocity varied according to the law $\sim E^{-2.1}$ [26]. For a spherical layer performing tidal oscillations with a frequency $\sigma_{\text{tide}} = 0.88$, scaling $\sim E^{-3/2}$ was obtained numerically, and for frequency $\sigma_{\text{tide}} = 1$ the velocity decreased as the inverse square root of Ekman's number, $\sim E^{-1/2}$ [16,18].

Figure 9 shows the distribution of averaged velocity over the libration frequency σ at Ekman number $E = 2.4\times10^{-3}$. The circles correspond to the flow associated with inertial modes, and the rhombuses correspond to the corner flow at distance $|2z/L| = 0.8-1.0$. In contrast to the case presented in Fig. 5, only three main maxima corresponding to the modes {2,2}, {2,1}, and {4,1} are observed. An increase in E leads to the expansion of the frequency boundaries of the main modes of existence and the simultaneous dissipation of higher-order modes. For example, at libration frequencies σ, corresponding to the modes {4,2} and {6,2}, a pulsating flow corresponding to the modes {2,1} and {4,1} occurs. In turn, a change in the regime of oscillating fluid motion leads to a transformation of the steady circulation structure.

Note that, in the above case, the shape of the curve for the corner flow (rhombuses in Fig. 9) repeats the form of the dependence $V(\sigma)$. The velocity V_c can exceed the velocity V several times, which is especially noticeable at libration frequencies $\sigma > 1.3$. This can be explained by the fact that, with an increase in the mode number, the amplitude of the pulsating fluid motion rapidly decreases with the distance from the ends. As observations show for mode {6,1}, the value of vorticity in the vortices located at a distance $|2z/L| \approx 0.2$ is significantly less than that in vortices

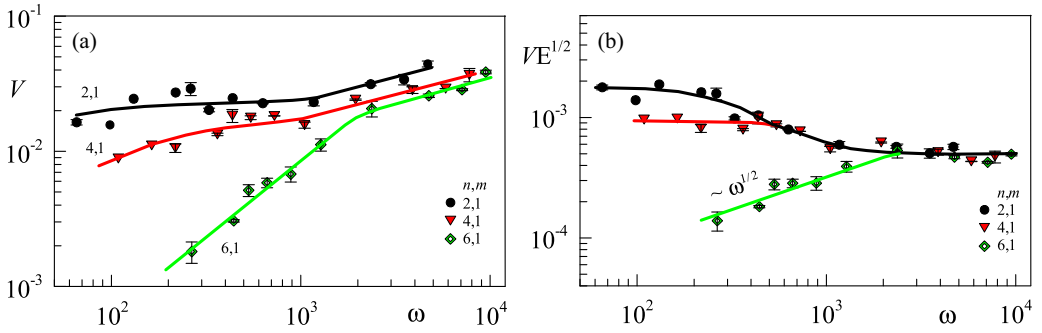

FIG. 10. Dependence of averaged velocity on the dimensionless frequency of fluid oscillations, ω.

on the periphery. Moreover, the flow near the cavity ends is determined by the combined action of two mechanisms (rotational oscillations of the cavity and inertial mode), resulting in the velocity V_c being about three times higher than V.

IV. DISCUSSION

In the case of small oscillation amplitudes, the mechanism of the steady circulation generation is connected to the heterogeneity of the oscillating flow in the Stokes boundary layer close to the side wall of the cavity. Against the background of fluid oscillations excited by the inertial mode, a system of averaged toroidal vortices occurs. As experiments show (Figs. 3 and 6), the steady flow structure strongly depends on the dimensionless oscillation frequency $\omega = \Omega_{\text{lib}} R^2/\nu \sim R^2/\delta^2$, where δ is the Stokes layer thickness. The dependence of the averaged velocity V on ω is presented in Fig. 10(a). In the range of high frequencies ($\omega > 2\times10^3$), where the thickness of the dynamic Stokes layer is small compared with the cavity size, a monotonic increase in the velocity V according to a power law is observed. Moreover, the smaller the axial wave number of the inertial mode $\{n, 1\}$, the greater is the flow velocity. With a decrease in ω the thickness of the boundary layers increases and at $\omega < 2\times10^3$ the scaling changes. Meanwhile, for various libration frequencies σ the rate of the flow velocity change with ω is different.

Because of the dependence shown in Fig. 8 for the limit of low Ekman numbers, let us plot the parameter $VE^{1/2}$. As experiments show, in the range of Ekman numbers $E = 10^{-4}-10^{-2}$ and different axial wave numbers of the modes, the results are consistent on the plane of the parameters $\omega, VE^{1/2}$ [Fig. 10(b)]. It can be seen that, in the high-frequency limit, the parameter $VE^{1/2}$ reaches an asymptotic value 5×10^{-4}. When decreasing dimensionless frequency ($\omega < 2\times10^3$), the fluid velocity begins to depend on the inertial mode number, which is due to the effect of the corner flows. Therefore at wave numbers $\{2,1\}$ and $\{4,1\}$ the velocity $VE^{1/2}$ initially monotonically increases, and at $\omega < 2\times10^2$ gradually reaches its maximum value. The fluid velocity in the cavity corners is presented at Fig. 11. It is seen that independently of the libration frequency all experimental results are described by one dependence. At high ω the velocity of the averaged flow in the cavity corners is higher than in vortices associated with inertial oscillations of the liquid [Fig. 10(b)]. With a decrease in the dimensionless frequency at $\omega < 8\times10^2$, a monotonic increase in the flow rate to the value $V_cE^{1/2} \approx 10^{-3}$ is observed. Likewise the steady circulation intensity increases for modes $\{2,1\}$ and $\{4,1\}$. Moreover, in the range of moderate dimensionless frequencies ($\omega < 4\times10^2$) the velocity values $V_cE^{1/2}$ and $VE^{1/2}$ take close values. This indicates that the corner flows lead to increase in the velocity of the flow excited by inertial modes. In the libration frequencies region, where there are no inertial oscillations ($\sigma = 2$), the velocity of corner flows also varies with the dimensionless frequency. Observations show that, despite a significant increase in the value of the parameter $V_cE^{1/2}$ at $\omega = (4-8)\times10^2$, a qualitative change in the corner flow structure does not occur.

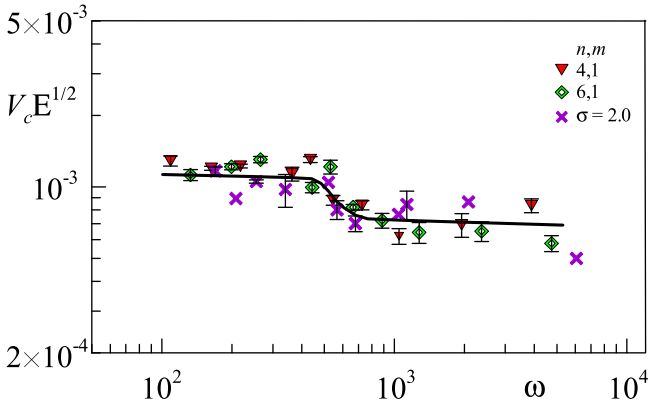

FIG. 11. The velocity of corner flow versus the dimensionless frequency ω.

The most interesting result is in the range of moderate dimensionless frequencies for the mode {6,1} [Fig. 10(b)]. Since attention was paid to the flow far from the cavity ends, corner vortices did not affect the measurement results. This means that the averaged velocity in these vortices is determined only by the amplitude of the pulsating flow in the fluid bulk. As experiments show, the decrease in ω leads to viscous flow dissipation according to the law $VE^{1/2} \sim \omega^{1/2}$. Given that the frequency of librations is defined as $\sigma = \Omega_{\rm lib}/\Omega_{\rm rot}$, and the amplitude $\varepsilon = \Delta\varphi\sigma$, we can get that

$$VE^{1/2} = \left|\bar{u}_z^m\right| E^{1/2}/(\Delta\varphi^2\Omega_{\rm lib}R\sigma). \tag{3}$$

This means that the dimensionless velocity of the steady flow is described by the expression

$$\left|\bar{u}_z^m\right|/\tilde{u} = 10^{-5}(\Delta\varphi\omega\sigma^{1/2}), \tag{4}$$

where $\tilde{u} \equiv \Delta\varphi\Omega_{\rm lib}R$ is the amplitude of the velocity of the oscillating fluid motion. Taking into account that in these experiments the frequency of librations σ does not change, we can conclude that the velocity in the central vortices is completely determined by the dimensionless frequency and does not depend on the Ekman number:

$$\left|\bar{u}_z^m\right|/\tilde{u} \sim \omega. \tag{5}$$

It is interesting that this result agrees well with the analysis of the steady flow excited by rotational oscillations of a cavity with a periodically deformed elastic wall [24]. In the mentioned studies, the average rotation of the cavity was equal to zero, while in the low-frequency limit the scaling for the velocity of the averaged flow was $|\bar{u}_z^m|/\Delta\varphi^2\Omega_{\rm rot}R \sim \omega$. Note that a linear decrease in speed with frequency ω was observed only at relatively large values of Ekman numbers, $E > 6\times10^{-4}$.

V. CONCLUSIONS

Steady circulation excited by the oscillating motion of a fluid in a nonuniformly rotating cylinder is investigated experimentally. The case of librations—harmonic oscillations of the rotation rate according to the law $\sim\varepsilon\sin(\Omega_{\rm lib}t)$—is considered. It is shown that the flow structure substantially depends on the libration frequency $\sigma = \Omega_{\rm lib}/\Omega_{\rm rot}$. In the case when the frequency is $\sigma > 2$, the oscillations lead to the appearance of corner flow, i.e., pairs of toroidal vortices near the junction of the side and end walls of the cylinder. In the case when $\sigma \leqslant 2$ at certain libration frequencies, an intense oscillating motion of the liquid—inertial modes—occurs. The inertial modes lead to the excitation of additional steady circulation in the Stokes boundary layer on the cylinder side wall in the form of a system of toroidal vortices. The velocity of the flow in the vortices changes nonmonotonically with frequency σ, experiencing a series of extrema corresponding to the resonant

excitation of the inertial mode. Thus, the flow structure close to the side wall of the cavity has a three-dimensional form.

The structure of the flow at a fixed value of σ highly depends on the dimensionless fluid oscillation frequency $\omega = \Omega_{\text{lib}} R^2/\nu$, determining the ratio of the cavity size to the thickness of the dynamic Stokes layer. Therefore in the case of high ω the number of averaged vortices is described by the expression $n + 2$, where n is the axial wave number of the inertial mode. An additional pair of vortices is due to the presence of corner flow. The transverse size of the vortices is limited by several thicknesses of the Stokes boundary layer, and the axial size is comparable to the size of the oscillating vortices. The exception is the area near the cavity ends. The matching of the sizes of the averaged and oscillating vortices indicates the fact that the generation mechanism of these flows is associated with nonlinear effects in the Stokes layer due to inhomogeneous oscillating fluid motion. In the high-frequency limit, independently of the inertial mode number, the flow velocity does not depend on ω and is completely determined by the parameter $VE^{1/2} = |\bar{u}_z^m| E^{1/2}/\Omega_{\text{rot}} R\varepsilon^2$, where E is the Ekman number.

With a decrease in the dimensionless frequency, the thickness of the boundary layers increases, resulting in a transformation of the flow structure. In the case of modes {2,1} and {4,1} the central vortices gradually move to the periphery, interacting with the corner flow. Thereby, near the ends, the resulting flow is a superposition of flows caused by two different mechanisms: rotational oscillations of the cavity and resonant fluid oscillations. With a further decrease in the dimensionless frequency, the size of the averaged vortices becomes comparable with the cavity size.

At the oscillation frequency corresponding to the mode {6,1} the vortices most distant from the cavity ends are not affected by the corner flow. As a result, the velocity in these flows is determined only by the amplitude of the oscillating motion in the fluid bulk. Experiments performed at a fixed value of σ in the range of Ekman numbers $E = 6\times(10^{-4}-10^{-3})$ showed that the velocity of the steady circulation changes with dimensionless frequency according to the law $|\bar{u}_z^m|/\Delta\varphi^2\Omega_{\text{rot}} R \sim \omega$.

Since oscillations are typical for planetary bodies, the question about the possibility of averaged vorticity generation in the boundary layers of liquid cores or subsurface oceans is relevant. For planets the Ekman numbers are very small ($E \sim 10^{-14}$ [27]), while the source of resonant inertial oscillations of the liquid can be not only longitudinal librations, but also tidal deformations, as well as buoyant oscillations with the natural frequency of the solid core. The results of the present work are limited to a narrow range of dimensionless frequencies $\omega = 10^2-10^4$ (Fig. 10); nevertheless, at $\omega > 2\times10^3$ the flow velocity reaches an asymptotic value. It can be assumed that, after extrapolating the data to $\omega = \sigma/E \sim 10^{14}$, the rate of steady circulation will also be determined by the parameter $VE^{1/2}$. Despite the fact that the present study was conducted in a cylindrical geometry, one can expect the emergence of similar averaged effects in the boundary layers in spherical geometry. This is indicated by the experimental results described in [20]. The reflection of inertial wave beams from the inner wall of the spherical cavity is accompanied by the appearance of azimuthal axisymmetric structures at different latitudes. Therefore, in future studies, it will be interesting to pay attention to steady boundary layer circulation excited by inertial modes in a spherical cavity.

ACKNOWLEDGMENTS

The research was supported by a grant of the President of the Russian Federation (Project No. MK-1994.2018.1). The author acknowledges support as a member of the leading scientific school (agreement with the Ministry of Education and Science of the Perm region No. C-26/1191)

[1] N. Riley, Steady streaming, Annu. Rev. Fluid Mech. **33**, 43 (2001).

[2] H. P. Greenspan, *The Theory of Rotating Fluids* (Cambridge University Press, Cambridge, 1968).

[3] M. Le Bars, D. Cébron, and P. Le Gal, Flows driven by libration, precession, and tides, Annu. Rev. Fluid Mech. **47**, 163 (2015).

[4] F. H. Busse, Mean zonal flows generated by librations of a rotating spherical cavity, J. Fluid Mech. **650**, 505 (2010).
[5] M. A. Calkins, J. Noir, J. D. Eldredge, and J. M. Aurnou, Axisymmetric simulations of libration-driven fluid dynamics in a spherical shell geometry, Phys. Fluids **22**, 086602 (2010).
[6] J. L. Margot, S. J. Peale, R. F. Jurgens, M. A. Slade, and I. V. Holin, Large longitude libration of Mercury reveals a molten core, Science **316**, 710 (2007).
[7] P. C. Thomas, R. Tajeddine, M. S. Tiscareno, J. A. Burns, J. Joseph, T. J. Loredo, P. Helfenstein, and C. Porco, Enceladus's measured physical libration requires a global subsurface ocean, Icarus **264**, 37 (2016).
[8] C. Y. Wang, Cylindrical tank of fluid oscillating about a steady rotation, J. Fluid Mech. **41**, 581 (1970).
[9] F. H. Busse, Zonal flow induced by longitudinal librations of a rotating cylindrical cavity, Physica D **240**, 208 (2011).
[10] J. Noir, M. A. Calkins, M. Lasbleis, J. Cantwell, and J. M. Aurnou, Experimental study of libration-driven zonal flows in a straight cylinder, Phys. Earth Planet. Inter. **182**, 98 (2010).
[11] A. Sauret, D. Cébron, M. Le Bars, and S. Le Dizès, Fluid flows in a librating cylinder, Phys. Fluids **24**, 026603 (2012).
[12] L. Messio, C. Morize, M. Rabaud, and F. Moisy, Experimental observation using particle image velocimetry of inertial waves in a rotating fluid, Exp. Fluids **44**, 519 (2008).
[13] J. Boisson, C. Lamriben, L. R. M. Maas, P. Cortet, and F. Moisy, Inertial waves and modes excited by the libration of a rotating cube, Phys. Fluids **24**, 076602 (2012).
[14] I. D. Borcia, G. V. Abouzar, and U. Harlander, Inertial wave mode excitation in a rotating annulus with partially librating boundaries, Fluid Dyn. Res. **46**, 041423 (2014).
[15] K. Wu, B. D. Welfert, and J. M. Lopez, Librational forcing of a rapidly rotating fluid-filled cube, J. Fluid Mech. **842**, 469 (2018).
[16] A. Tilgner, Zonal Wind Driven by Inertial Modes, Phys. Rev. Lett. **99**, 194501 (2007).
[17] C. Morize, M. Le Bars, P. Le Gal, and A. Tilgner, Experimental Determination of Zonal Winds Driven by Tides, Phys. Rev. Lett. **104**, 214501 (2010).
[18] B. Favier, A. Barker, C. Baruteau, and G. Ogilvie, Nonlinear evolution of tidally forced inertial waves in rotating fluid bodies, Mon. Not. R. Astron. Soc. **439**, 845 (2014).
[19] V. Kozlov and D. Polezhaev, Flow patterns in a rotating horizontal cylinder partially filled with liquid, Phys. Rev. E **92**, 013016 (2015).
[20] V. G. Kozlov, N. V. Kozlov, and S. V. Subbotin, Steady flows excited by circular oscillations of free inner core in rotating spherical cavity, Eur. J. Mech. B Fluids **58**, 85 (2016).
[21] S. Subbotin and V. Dyakova, Inertial waves and steady flows in a liquid filled librating cylinder, Micrograv. Sci. Technol. **30**, 383 (2018).
[22] W. Thielicke and E. J. Stamhuis, PIVlab–Time-Resolved Digital Particle Image Velocimetry Tool for MATLAB, version 1.41, 2016.
[23] M. Klein, T. Seelig, M. V. Kurgansky, Abouzar Ghasemi V., I. D. Borcia, A. Will, E. Schaller, C. Egbers, and U. Harlander, Inertial wave excitation and focusing in a liquid bounded by a frustum and a cylinder, J. Fluid Mech. **751**, 255 (2014).
[24] V. G. Kozlov, S. V. Subbotin, and R. R. Sabirov, Steady flows in deformed elastic sphere subject to rotational oscillations, Phys. Fluids **30**, 093606 (2018).
[25] R. Repetto, J. H. Siggers, and A. Stocchino, Steady streaming within a periodically rotating sphere, J. Fluid Mech. **608**, 71 (2008).
[26] A. Sauret, M. Le Bars, and P. Le Gal, Tide-driven shear instability in planetary liquid cores, Geophys. Res. Lett. **41**, 6078 (2014).
[27] J. Noir, F. Hemmerlin, J. Wicht, S. M. Baca, and J. M. Aurnou, An experimental and numerical study of librationally driven flow in planetary cores and subsurface oceans, Phys. Earth Planet. Inter. **173**, 141 (2009).